The CRISPR Journal
Volume 3, Number 3, 2020
Mary Ann Liebert, Inc.
DOI: 10.1089/crispr.2019.0066

The CRISPR Journal

RESEARCH ARTICLE

A Flexible, Pooled CRISPR Library for Drug Development Screens

Maximilian Blanck,[1] Milka B. Budnik-Zawilska,[1] Steven R. Lenger,[2] John E. McGonigle,[1] Glynn R.A. Martin,[1] Carlos le Sage,[1] Steffen Lawo,[3,*] Helen N. Pemberton,[1] Gaganpreet S. Tiwana,[1] David A. Sorrell,[1,*] and Benedict C.S. Cross[4,*]

Abstract

Functional genomic screening with CRISPR has provided a powerful and precise new way to interrogate the phenotypic consequences of gene manipulation in high-throughput, unbiased analyses. However, some experimental paradigms prove especially challenging and require carefully and appropriately adapted screening approaches. In particular, negative selection (or sensitivity) screening, often the most experimentally desirable modality of screening, has remained a challenge in drug discovery. Here we assess whether our new, modular genome-wide pooled CRISPR library can improve negative selection CRISPR screening and add utility throughout the drug development pipeline. Our pooled library is split into three parts, allowing it to be scaled to accommodate the experimental challenges encountered during drug development, such as target identification using unlimited cell numbers compared with target identification studies for cell populations where cell numbers are limiting. To test our new library, we chose to look for drug–gene interactions using a well-described small molecule inhibitor targeting poly(ADP-ribose) polymerase 1 (PARP1), and in particular to identify genes which sensitise cells to this drug. We simulate hit identification and performance using each library partition and support these findings through orthogonal drug combination cell panel screening. We also compare our data with a recently published CRISPR sensitivity dataset obtained using the same PARP1 inhibitor. Overall, our data indicate that generating a comprehensive CRISPR knockout screening library where the number of guides can be scaled to suit the biological question being addressed allows a library to have multiple uses throughout the drug development pipeline, and that initial validation of hits can be achieved through high-throughput cell panels screens where clinical grade chemical or biological matter exist.

Introduction

Pooled CRISPR knock-out (CRISPRko) screens have successfully identified genome-wide collections of essential genes,[1–4] as well as mechanisms of drug resistance and associated biomarkers.[5–7] However, this technology is also a valid tool for the identification of biomarkers of drug sensitivity where perturbations increase the toxicity of a drug or another insult. Sensitivity screening, also known as negative selection screening, requires the identification of the loss of a key genotype or phenotype from the experimental population. This is a more challenging screen modality, as the experiment is looking to find the rarer event (i.e., loss of certain cell populations), which is contingent upon high penetrance of gene disruption and typically results in more complex datasets where the signal-to-noise ratio is greater.[8] Consequently, relatively fewer negative selection drug–gene interaction screens have been published,[9–12] in contrast to many positive selection screens.[13–15] While the rapid development of pooled lentivirus and deep-sequencing-led approaches have allowed us and others to exploit the positive selection approach in target identification (ID), drug mechanism of action analysis, and patient stratification focused screens, adapted tools are required to adequately capture the reciprocal interest in sensitivity screening.

[1]*Horizon Discovery, Cambridge, United Kingdom;* [2]*Horizon Discovery, Lafayette, Colorado, USA;* [3]*Max Planck Institute for Biology of Ageing, Cologne, Germany;* [4]*PhoreMost Ltd., Cambridgeshire, United Kingdom.*

*Address correspondence to: *Benedict C.S. Cross, PhD, PhoreMost Ltd., Building 250, Babraham Research Campus, Cambridgeshire CB22 3AT, United Kingdom,* E-mail: benedict.cross@phoremost.com*; David A. Sorrell, PhD, Horizon Discovery, 8100 Cambridge Research Park, Cambridgeshire CB25 9TL, United Kingdom,* E-mail: david.sorrell@horizondiscovery.com; *Steffen Lawo, PhD, Max Planck Institute for Biology of Ageing, Cologne, Germany, P.O. Box 41 06 23,* E-mail: slawo@age.mpg.de

Dual-direction and combined screening approaches have been of great value in improving screen datasets for negative selection screens[6,16] These screens require an additional arm that provides gain-of-function information, and whilst powerful, they are experimentally complex and might not provide high-sensitivity loss-of-function genetic disruptions needed for rapid drug development. Adapting pooled phenotypic approaches[17] and simple haploid genetics[18,19] has also increased screen power in some cases, but these specific examples required that the cell death pathways can be identified in a time-resolved way or use a restrictive cell line background, respectively, and therefore have limited generalized applicability. Much progress has been made in improving both the penetrance and the precision of CRISPR-based tools for screening, including the development of new algorithms to better predict guide sequences and modifications to the molecular infrastructure to increase editing rates,[14,20,21] but robust screen outcomes for negative selection remain challenging. A common feature of existing algorithms for guide target site identification is the use of gene essentiality datasets to train them. However, the reductionist tendency of these algorithms often yields smaller, low complexity libraries.

Recognizing that screen success rarely uses a one-size-fits-all approach, here we have built a flexible pooled screening CRISPRko library that is partitioned into three parts to allow library design and complexity to meet the experimental challenges of a given individual screen. For instance, resistance screening could be viewed as a relatively low-risk endeavor in most cases, and screens can be successfully conducted using a lower complexity library with four guides targeting each gene. By contrast, negative selection screens require greater experimental power for robust hit ID, so a library with six or eight guides per gene could be deployed to accommodate the need for greater experimental power. We tested our library design of four guides per gene, six guides per gene, or eight guides per gene in a negative selection screen to identify genes that interact and specifically sensitize cells to the poly(ADP-ribose) polymerase 1 (PARP1) inhibitor olaparib. Some of the hits identified in the four-, six- and eight-guide library components are validated by high-throughput cell panel screening.

Materials and Methods

Cell lines

HT-29 cells (American Type Cell Culture) were cultured in McCoy's supplemented with 10% fetal bovine serum (all supplied by Gibco UK). Cells were routinely checked for mycoplasma and identity verified by short tandem repeat (STR) analysis.

Library generation

We generated three pooled, whole-genome guide RNA libraries using the guide RNA design algorithms from the Edit-R tool (Horizon Discovery).[22] Each single guide RNA (sgRNA) was synthesized (CustomArray, Inc.) using a modified trans-activating CRISPR RNA sequence, as described in Chen *et al.*[23] and Cross *et al.*[18] (5′-GTTTAAGAGCTATGCTGGAAACAGCATAGCAAGTT-3′). An all-in-one lentivirus plasmid vector was used comprising a selection marker (puromycin resistance), the expression cassette for Cas9 and the sgRNA sequence. Each pooled sgRNA library was cloned into the vector backbone using a Gibson Assembly Master Mix kit (New England BioLabs) in accordance with the manufacturer's instructions. Library plasmids were purified using a Qiagen Plasmid Plus purification system in accordance with the manufacturer's instructions.

Lentivirus production

Lentivirus was produced as described in Le Sage *et al.*[6]

Cell transduction and screening protocol

Cell culture and screening was conducted as described in Le Sage *et al.*[6] Deviations from the previously described protocol were the use of HT-29 cell line in the current study. A total of 1.5×10^8 cells were transduced; 48 h after library transduction, transduced and nontransduced cells were treated with puromycin at a final concentration of 0.6 μg/mL. Once selection was complete, puromycin was removed and cell populations were divided for treatments and replicates and maintained in multiple five-layer flasks (Falcon), counted, and reseeded at 5.5×10^7 cells per treatment every 3–4 days with appropriate treatments. Final pellets were harvested after 12 doublings of cells treated with DMSO. Genomic DNA was extracted using QIAamp DNA Blood Maxi kit (Qiagen). DNA concentration was determined using a Nanodrop spectrophotometer and at least 230 μg of genomic DNA for each sample was then amplified by PCR to generate amplicons of the sgRNA cassette using a forward primer, TC GTCGGCAGCGTCAGATGTGTATAAGAGACAGU–[variable]–TGTGGAAAGGACGAAACACC; and a reverse primer, GTCTCGTGGGCTCGGAGATGTGTA TAAGAGACAGGATCAATTGCCGACCCCTCC. These amplicon samples were purified using Agencourt beads (Beckman) and deep sequenced on an Illumina NextSeq platform (Microsynth AG).

Data analysis

Raw next-generation sequencing libraries were evaluated for quality using FASTQC version 0.11.5. (Babraham Institute; Cambridge, UK).[24] Guide counts were obtained using an in-house customized version of k-mer counting, which took into account guide staggering from the experimental protocol. Briefly, guide-length fragments were trimmed and hashed before mapping with exact string counts from each file to provide raw counts for each guide found in the library. Guide counts were then normalized within each group (median based) and Log2 fold change was calculated to determine the change in abundance of each guide in each sample. DrugZ was used as the drug-interaction scoring tool, as described previously.[25,26] Network analysis was conducted using EsyN and HumanMine with physical interaction.[27]

Cell panel screening

Cell lines were grown in vendor recommended culture medium and STR-typed to verify identity. Cells were seeded into 384-well assay plates and compounds added after 24 h using a nine-point titration plus untreated control for the single agent assays or a 6×6 optimized dose matrix for the combinations. After a further 6 days of incubation, cell viability was assessed using CellTiter-Glo 2.0 (Promega). A baseline T0 measurement (at time of drug of addition) was also taken to enable calculation of growth inhibition, which enables the differentiation between cytostasis and cytotoxicity. Single agent responses were analyzed by calculating the area under the dose–response curve (response area) and combinations were analyzed using synergy score which was calculated using the Loewe additivity model using Horizon's proprietary Chalice Analyzer software. (For detailed methods see Kondo *et al.* 2002.[28]) Pharmacogenomic analysis of response was performed using the mRNA expression and CRISPRko gene dependency data obtained from the Cancer Dependency Map (Depmap) portal release 2019q3. Correlation between drug response and PARP1 expression was analyzed by Pearson correlation. Cells were ranked according to drug sensitivity using Response Area and the top and bottom quartiles were assigned as responders or nonresponders, respectively. Significant differences in gene dependencies between these two populations were then identified using Fisher's exact test. Network analysis of the top 250 genes that sensitive cell lines were more dependent on was performed using EsyN and BioGRID with physical interaction,[27] and functional annotation and clustering was performed using the DAVID Bioinformatics Tool v6.8.[29]

Results

We partitioned the guides in our library for synthesis across three independent arrays: one containing four guides (LibA), and a further two arrays containing two guides per gene each (LibB and LibC). When these library subsets are combined at the plasmid level in, they generate a library in which a total of eight guides targets each gene (Fig. 1). This approach facilitates screening using a library consisting of four, six, or eight guides, in accordance with the desired complexity. For the proof of concept screen, each library plasmid was combined in equimolar concentrations and packaged as a single lentiviral pool with eight guides per target gene (LibABC).

We tested this ABC pooled library in a drug–gene interaction screen using the PARP1 inhibitor olaparib (Fig. 1A). PARP1 inhibitors are well studied, and cells that have compromised BRCA1 or BRCA2 function are known to be sensitive to these inhibitors. However, other studies indicate the existence of BRCAness, where increased sensitivity to PARP1 inhibitors is evident in the absence of BRCA1 or BRCA2 mutations.[30] Moreover, mechanisms of response to PARP1 inhibition in tumors is etiologically dynamic and can result from diverse effects, including increasing DNA lesions resulting from loss-of-function of PARP1 and trapping of PARP at the loci of DNA damage.[31] Thus, our screen should be able to identify known sensitivity mechanisms to olaparib to check that our library is effective, and to potentially identify additional mechanisms of sensitivity.

HT-29 cells are a common-use colorectal carcinoma laboratory screening model, and these cells were infected with the ABC library at a low multiplicity of infection followed by antibiotic selection to eliminate untransduced cells. Following selection, replicate populations of cells were split off and treated with either DMSO (vehicle control) or a dose of 10 μM olaparib. Importantly, after each treatment phase (one passage), cells in each replicate were harvested and counted to monitor treatment response and maintain optimal dose effect. This was deemed to be a response rate of 20%–30% growth inhibition compared with control and was rigorously optimized in pilot experiments (data not shown; Fig. 1C). This growth inhibition provides both confidence of target engagement (which results in loss of cell viability) and a large assay window into which increments of effect resulting from CRISPR perturbation can be measured, allowing a suitable negative selection screening output.

Following the completion of the screen treatment phase, which was terminated at 12 population doublings of the vehicle control, samples were harvested and genomic DNA was extracted and subjected to amplicon-based

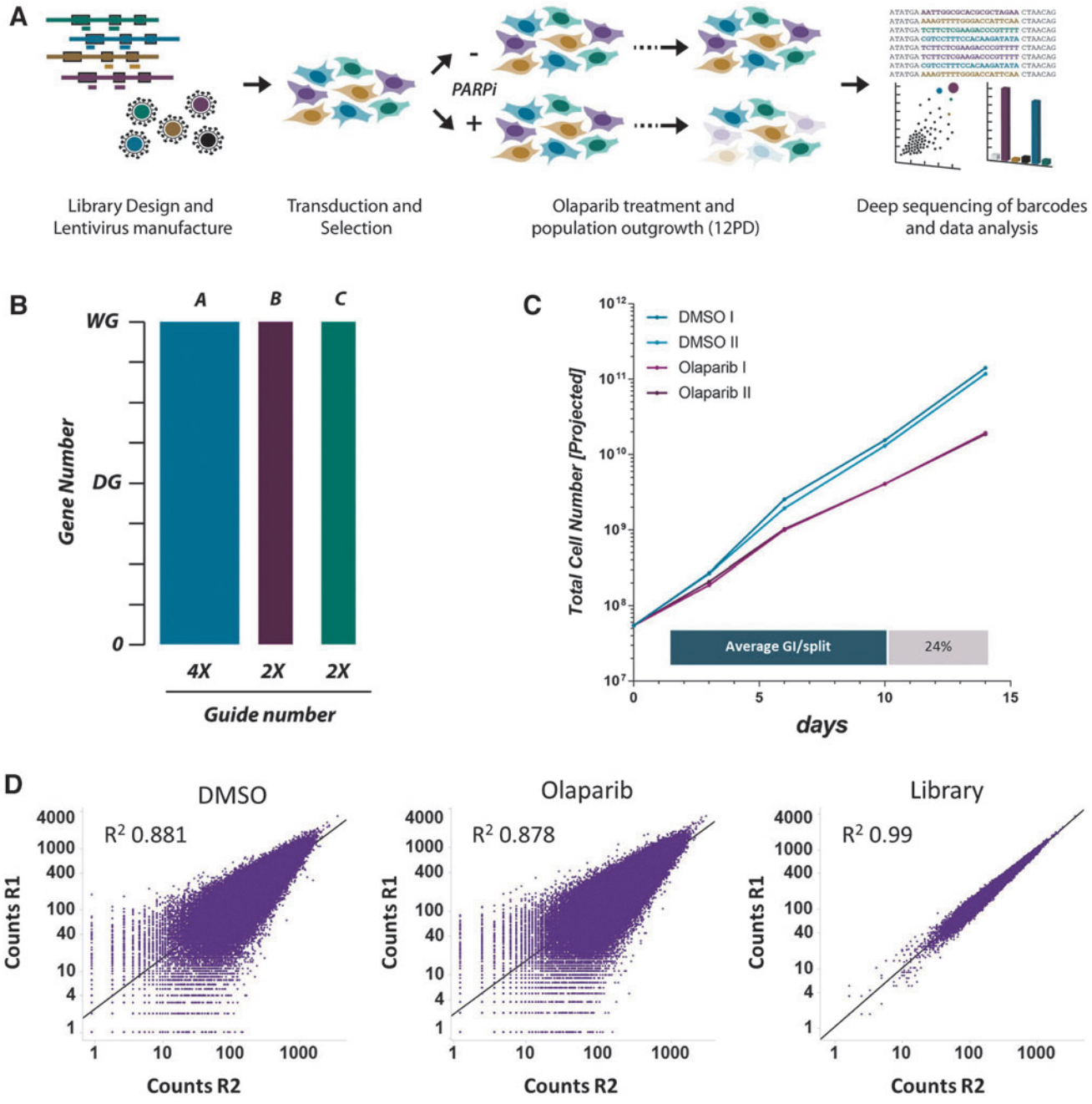

Fig. 1. **(A)** Schematic for negative selection drug-gene interaction screening. **(B)** Design of a flexible library for screening. A total of 18,500 genes were targeted, with guides targeting each gene split between three libraries: A, B, and C. LibA contains 76,886 guides; LibB contains 36,871 guides; LibC contains 36,454 guides. Libraries are then combined to provide appropriate depth of screening for each campaign. **(C)** Growth tracking of cells in each replicate and for each treatment. An average GI (growth inhibition) was determined across all passages as 24%. Screening was conducted with the full, combined ABC library. **(D)** Replicate correlations were determined and reported by rank analysis. Plots show total log next-generation sequencing counts per guide. DG, [druggable genome]; DMSO, dimethyl sulfoxide; PARPi, [PARP1 inhibitor; olaparib]; WG, [whole-genome]; R1, [replicate 1]; R2, [replicate 2].

sequencing to quantitatively identify genotype abundance in each sample. Replicates were analyzed side by side and showed high levels of concordance (Fig. 1D). Genes were annotated for known control groups, and the vehicle control sample was compared to baseline sequencing files derived from the plasmid samples ahead of lentivirus production. As we included nontargeting guides, positive controls (essential genes) and negative controls (nonessential genes) in our library, this comparison with plasmid samples allows a thorough qualification of expected effects on cell survival and fitness resulting from gene perturbation. Analysis of these control groups at the population level showed the expected behavior where essential genes were robustly lost from the population over time (Fig. 2A). Gene-level analysis showed drop out of essential targets up to 64-fold in some cases (Log_2 −6); likewise, guide-level analysis showed low representation of all guides targeting essential genes at the screen endpoint. As expected, LibABC showed modest overall enrichment for non-targeting controls.[18] In silico comparison between each of the sub libraries was conducted to evaluate the performance of each module directly. This was determined by independent analysis of each of the library subsets and combinations thereof, to simulate the performance of a screen using LibA, LibAB and LibABC. The greatest overall drop-out and lowest variance of control essential genes was observed in the smallest library, LibA, as expected, since this library contains the highest-ranking guides (Fig. 2B). Interestingly, discovery of gene essentiality as measured by a receiver operating curve analysis was found to be robust with only two guides, but increasing guide numbers clearly improved this outcome (Fig. 2C).[32]

This result is reassuring for the quality control of the library. However, the identification of pan essential genes by CRISPRko is among the more straightforward of analytical tasks, since a defined list of expected essential genes exists. In order to explore the performance of our modular library in drug–gene interaction, we used the DrugZ analytical tool,[25] which for this data proved more sensitive than other methods, such as the more frequently used robust ranking aggregation tools (data not shown).[33] This analysis was conducted for each of the library modules. Discovery of sensitizing hits was surprisingly robust even with the low complexity LibA, which has four guides (Fig. 3A). We identified 39 hits with a false discovery rate <0.05 (Fig. 3B), including *ATM* and a large part of the Fanconi anemia (FA) pathway. Several other key agonists of DNA damage response (DDR) pathways such as *MUS81, XRCC1,* and *POLB* were also identified, which indicates a robust on-target effect in response to treatment with olaparib. All three components of ribonuclease H2 were found to be significantly depleted in the treated sample. More detailed guide-level analysis indicates a reproducible response for these top hits (Fig. 3C). These genes were also found as part of a previously published study that is similar to ours.[9] Comparing our data in HT-29 cells with the published data set[9] shows good concordance between the two studies (Fig. 3D).

Although hit ID was found to be robust even with the simulated lower complexity library, a substantial increase of hits was observed with increasing numbers of guides. Up to 58 hits were found with the eight-guide library. Importantly, whilst *BRCA1* was identified robustly in each library analysis, *PTEN* was found only when analyzing the screen with the eight-guide library (LibABC). Previous publications have indicated that cells lacking functional *PTEN* are more sensitive to PARP1 inhibitors,[34] and our data further supports these findings.

In addition to the analysis of genes that when lost sensitize to PARP inhibitors, we also used our data to look for resistance hits. Loss of *PARG* was a consistent hit found with all three simulated versions of the screen, with the highest representation of hits being evident with LibABC, which was able to identify PARP1 with substantially improved confidence (Fig. 3A). Overall, these observations illustrate the value of additional library complexity when looking for robust and maximum hit ID.

As our screen used a combined LibABC analyzed independently informatically, we sought additional validation for hits identified with each version of the component libraries. To do this, we used an orthogonal pharmacological cell panel screening approach. We ran a single agent screen with a viability readout following six days of drug treatment using a diverse panel of 326 cancer cell lines treated with olaparib and a second clinical-stage PARP inhibitor, talazoparib (BMN 673). The pattern of response across different tissue lineages was broadly similar for both compounds, and as previously reported, talazoparib was more potent than olaparib (Fig. 4A).[35] We used the publicly available genomic profile and genome-wide loss-of-function screening data for these cell lines in the DepMap portal to facilitate pharmacogenomic analysis of PARP inhibitor response. As expected, this revealed a significant positive correlation between PARP1 expression and inhibitor response (Fig. 4B), which is consistent with our finding that CRISPR-mediated knock out of PARP1 drives resistance to olaparib.

The integration of data obtained from drug sensitivity and loss-of-function screens is a valuable approach for identifying the underlying genes and pathways that

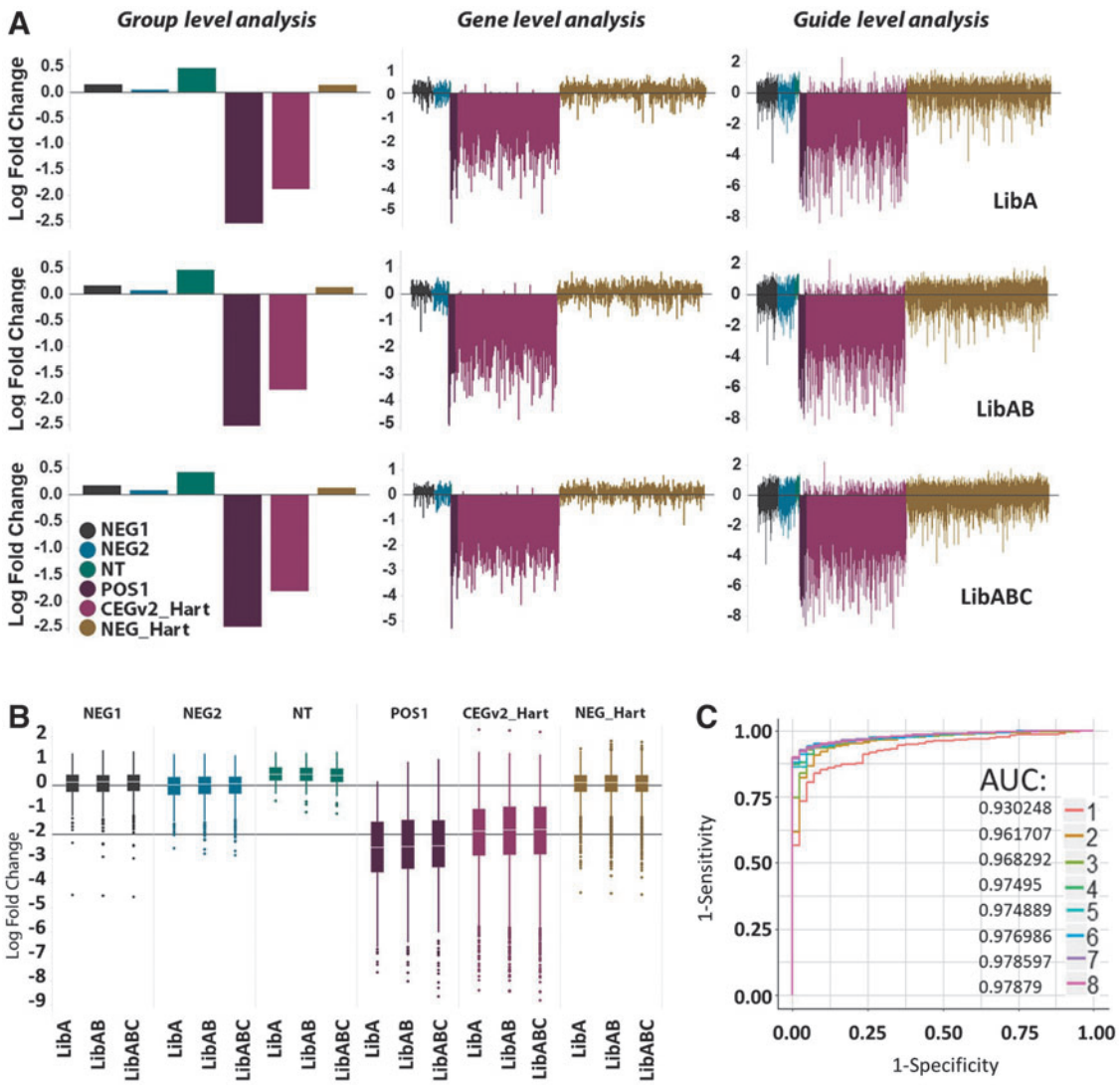

Fig. 2. **(A)** Control gene and guide performance was tracked by determining the log fold change in barcode (guide) abundance over time, from the plasmid baseline to the DMSO-treated endpoint. For each analysis, a group-level plot shows the median response of all control groups, whereas gene- and guide-level show higher resolution analysis of the same data. For the screen, analysis was conducted using either the full reference library (LibABC) or the smaller variants of this library, to evaluate how the reduced complexity libraries performed in comparison. Negative control groups show two alternative groups of putative neutral genes or the non-essential gene collection reported previously (NEG_Hart)[1]. Positive control gene group POS1 shows a limited group of genes previously reported as broadly essential,[18] whereas CEGv2_Hart annotates genes in the core essential collection.[1] NT indicates those guides with no targeting site. **(B)** Comparison of control groups by box plot for each library analysis. **(C)**. Receiver operator curve analysis of control group detection (essential genes vs. nonessential genes) for the screen when conducted with libraries targeting genes with only one guide all the way to the full LibABC approach, which contains eight guides per gene (numbers indicate guide number per gene). AUC, area under the curve.

govern drug responses.[2,36] Therefore, to elucidate genes and pathways that could be important in modulating the cellular response to olaparib, we further used the DepMap CRISPR-mediated whole-genome loss-of-function data to explore associations between our cell panel drug sensitivity dataset and gene dependencies. This was achieved by categorizing cell lines in the cell panel screen as responders or nonresponders and then systematically searching for significant differences in gene dependencies between the sensitive and resistant populations.

Strikingly, this revealed that olaparib sensitivity correlated with a greater dependence on genes or pathways that we and others identified using CRISPR sensitivity screens, including DNA damage and repair pathways and the spliceosome pathway (Fig. 4C and D).[9] Notably, the genes identified via the comparison of sensitive versus resistant cells included hits from the FA pathway that were identified using our lower complexity four-guide (*FANCG, FANCM* and *FAAP24*) and higher complexity eight-guide (*FANCE*) CRISPR libraries.

The identification of *ATM* (all libraries), *BRD2* (LibAB and LibABC), and *BCL2L1* (*BCL-XL*; LibABC only) as hits implicated the DDR pathway and *BET*- and *BCL2*-family members as potential therapeutic targets in combination with PARP1 inhibitors. To further validate these findings, we tested the ability of clinical-stage small molecule inhibitors against these targets to see whether there was synergy when used in combination with PARP1 inhibitors. We analyzed growth suppression in a panel of 10 cell lines that encompassed relevant cancer indications where PARP1 inhibitors are approved or are being evaluated in the clinic and two colorectal cancer cell lines, including HT-29, to compare with the data from our CRISPR screen (Fig. 5). The combinations of PARP inhibitors with ATM and other DDR pathway antagonists, such as inhibitors of *ATR, CHK1, CHK2* and *WEE1*, displayed strong synergy independent of which pathway node was inhibited (Fig. 5). The inclusion of multiple inhibitors against different parts of the pathway and the use of different inhibitors against the same target confirms that the observed synergy was pathway- and target-specific, rather than owing to any compound-specific off-target effect. The combination of PARP inhibitors with the *BET* and *BCL-2* inhibitors also exhibited robust and widespread synergy, although remarkably, synergy was only evident for the pan-*BCL-XL/2* inhibitor ABT-263 with relatively little being observed for the more *BCL-2*-selective compound ABT-199 (Fig. 5). This could indicate that synergy is primarily driven through inhibition of *BCL-XL* either alone or in combination with *BCL-2*. Although *PTEN*, a negative regulator of the PI3K pathway, was identified as a sensitizing hit in the CRISPR screen, no well-characterized small molecule antagonists for *PTEN* exist. We therefore evaluated the effects of PI3K pathway modulation by combining PARP antagonists with a PI3K pathway inhibitor. This combination was generally not synergistic and is consistent with the hypothesis that upregulation (via *PTEN* loss) rather than downregulation of the PI3K pathway might be a greater driver of sensitization to PARP inhibitors.

Overall, the data from the cell panel screens support the sensitization and resistance hits identified with our component ABC CRISPR library.

Discussion

We have developed a flexible and modular pooled CRISPRko screening library that can be used to tailor the power of each screen to the experimental or biological complexity required. To support the data generated using our new library we used high throughput combinatorial cell panel screens as an orthogonal validation tool. Our modular libraries use either four, six, or eight guides to decrease or increase the resolution of each screen, as appropriate. As a first demonstration of this approach, we explored a known challenging paradigm, negative selection screening. In contrast to positive selection or enrichment screening, this often more valuable approach is typically subject to greater noise resulting in poorer hit discovery. Our results indicate that the higher complexity library of eight guides per gene can be used for negative selection screening or where an experimental paradigm is anticipated to yield more noise. Examples of this would be pooled phenotypic screening with flow cytometry sorting endpoints or CRISPR screens conducted in complex cell systems, such as primary or induced pluripotent stem cell (iPSC)–derived tissues. Conversely, in experiments where cell numbers need to be kept low because

Fig. 3. **(A)** Drug–gene interaction analysis for each library analysis variant. DrugZ was used; a tool to assign statistical significance (*P*-values) and plotted in either the synthetic lethality (sensitivity) or suppression (resistance) direction against Log Fold Change. Hits are indicated (purple) and genes are colored by false discovery rate (FDR) value (blue <0.05). Genes are sized by normz (z-normalized magnitude of effect). **(B)** Network analysis (physical interaction) of hits passing an FDR threshold of 0.05 for analysis of the olaparib screen using either two, four, six, or eight guides per gene. In the LibABC analysis (eight guides), genes are colored by cross-over: green indicates genes that also scored in Zimmerman *et al.*[9] in all three cell lines; purple indicates sharing by only two lines and grey indicates order of significance for hits. BRCA1 is a hit network nexus and is colored gold for emphasis. **(C)** Guide distribution of key hits by log fold change at the endpoint relative to the DMSO-treated population. **(D)** Overlap of hits in screen published previously in alternative cell lines[9].

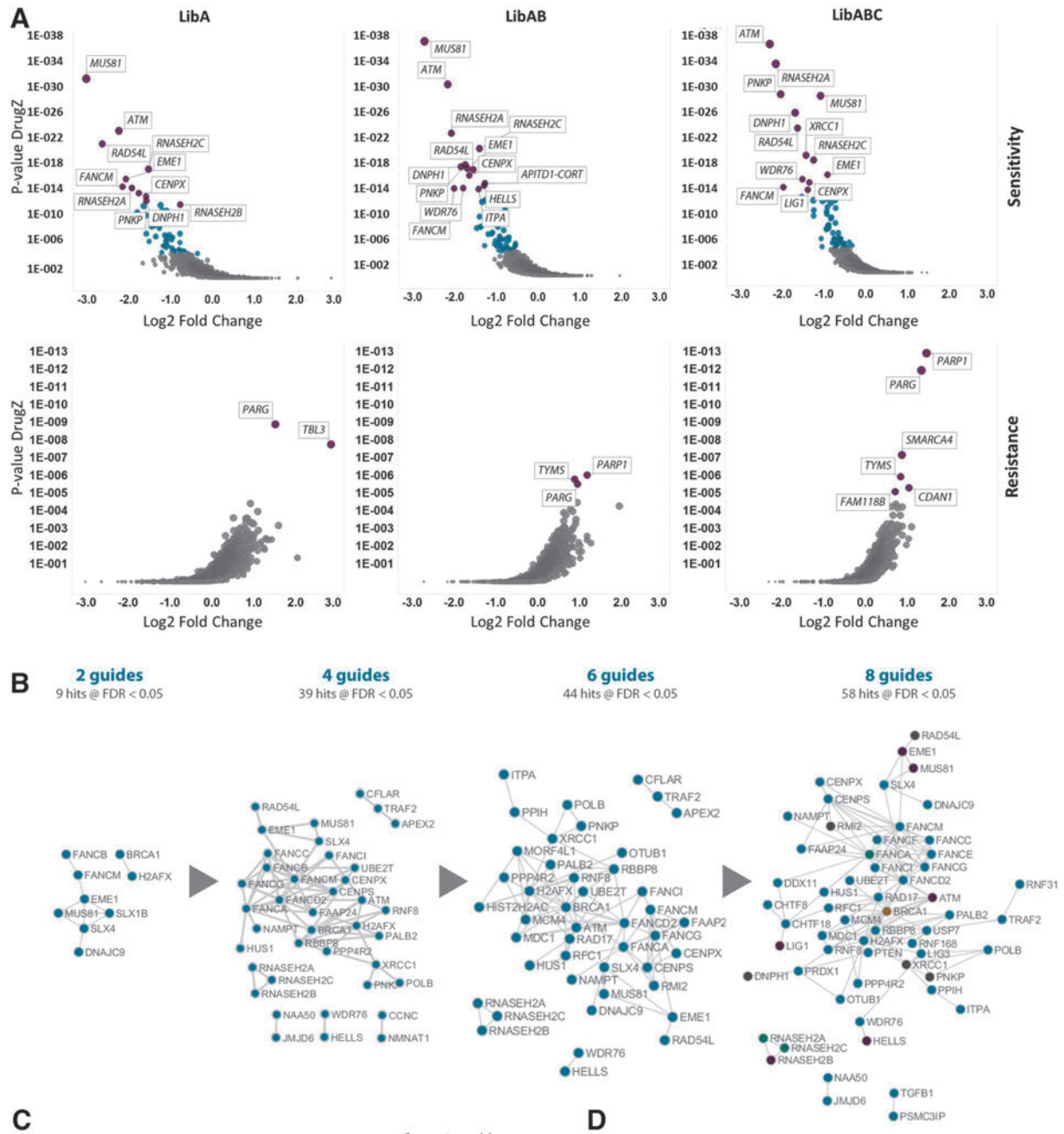
A
LibA
LibAB
LibABC
P-value DrugZ
Log2 Fold Change
Sensitivity
Resistance
MUS81
ATM
RNASEH2A
RNASEH2C
RAD54L
EME1
FANCM
CENPX
RNASEH2B
PNKP
DNPH1
APITD1-CORT
HELLS
WDR76
ITPA
FANCM
XRCC1
LIG1
PARG
TBL3
TYMS
PARP1
SMARCA4
FAM118B
CDAN1
B
2 guides
9 hits @ FDR < 0.05
4 guides
39 hits @ FDR < 0.05
6 guides
44 hits @ FDR < 0.05
8 guides
58 hits @ FDR < 0.05
C
Log Fold Change
ATM
BRCA1
FANCA
HELLS
LIG1
PTEN
RAD54L
RNASEH2A
RNASEH2B
RNASEH2C
D
Hela
SUM149PT
HT29
RPE1-hTERT
42
111
5
8
3
31
3
0
58
11
3
0
0
5
1

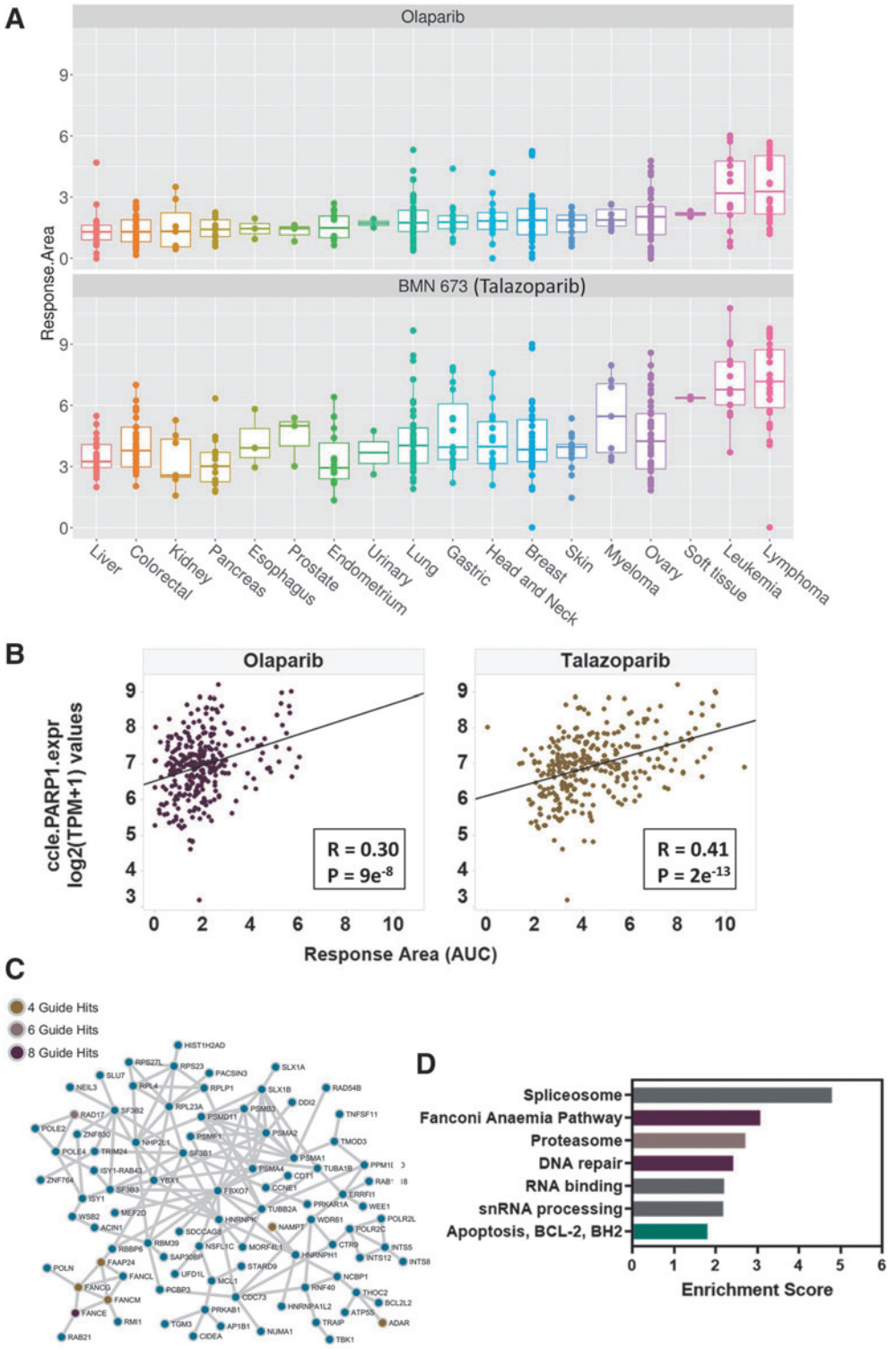

Fig. 4. Pharmacogenomic analysis of PARP inhibitor single agent responses across a cell panel. **(A)** Box plot showing PARPi responses across a 326-cancer cell line panel stratified by tissue type and ranked according to median values for olaparib. Cell viability was assessed following a 6-day treatment using CellTiter-Glo 2.0. A baseline T0 measurement (at time of drug addition) was taken to enable calculation of GI. Response area, which is the area under the dose response curve, was used as a measure of sensitivity to drug. **(B)** Correlation between PARPi responses and PARP1 gene expression across the cell panel. Pearson correlation statistics are shown. **(C)** Network analysis (with physical interaction) of genes on which olaparib sensitive cell lines are significantly more dependent relative to insensitive lines. Overlapping hits with the CRISPR screen are shown. **(D)** Functional annotation clustering analysis performed in the DAVID Bioinformatics tool of genes that olaparib sensitive cell lines are significantly more dependent relative to insensitive lines.

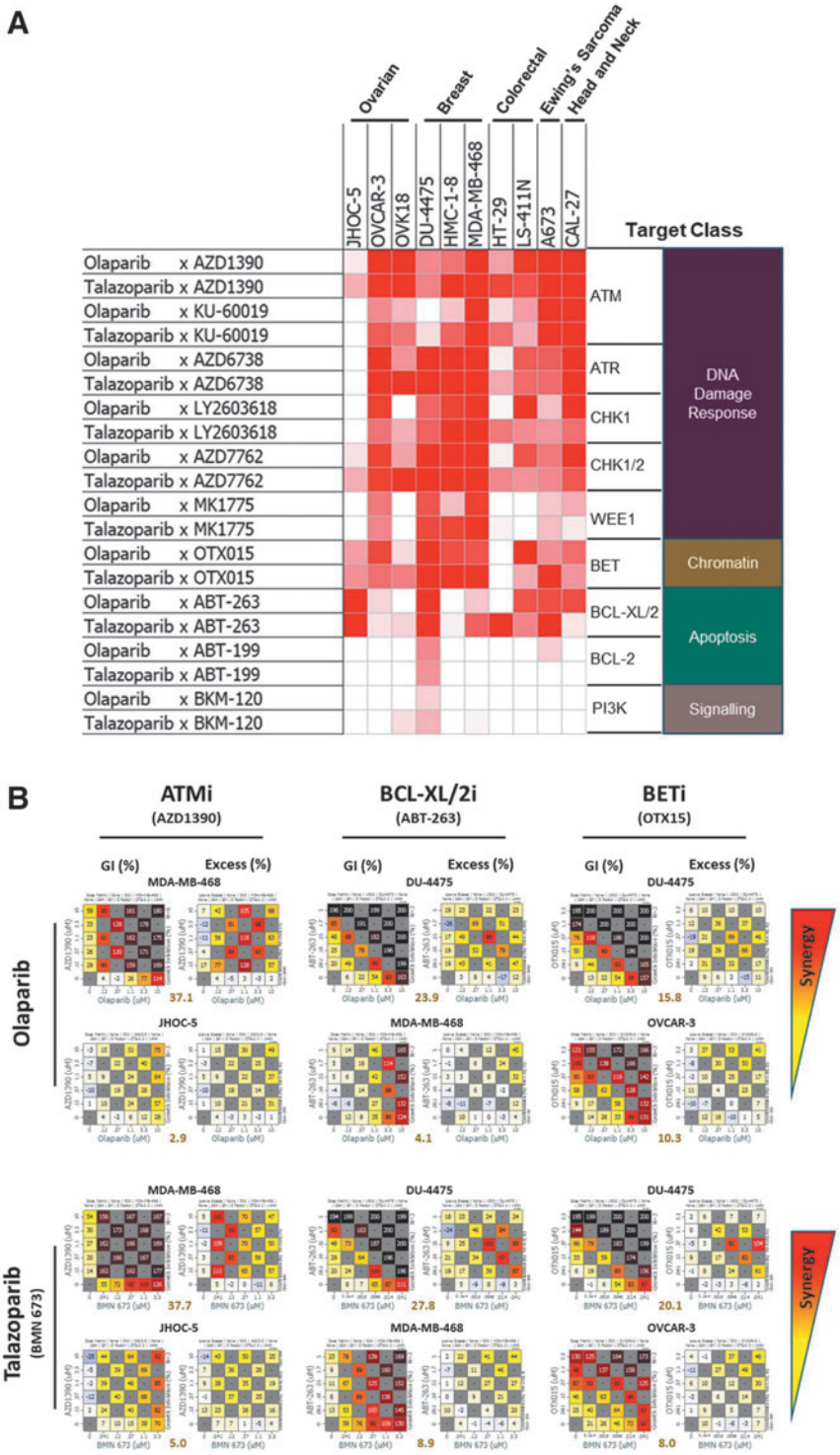

Fig. 5. Validation of CRISPR screening hits using combinations. **(A)** Heat-map representation of synergy scores from PARPi combinations across a panel of 10 cell lines. Cell viability was assessed following a 6-day treatment using CellTiter-Glo 2.0. A baseline T0 measurement (at time of drug addition) was taken to enable calculation of GI. The synergy scores were calculated from each dose matrix using the Loewe additivity model. **(B)** Representative dose matrices for combinations of PARP inhibitors with ATM, BCL-XL/2, and BET antagonists. For each combination, GI values (left matrix) and the Loewe excess values (right matrix) are shown. Loewe excess values are determined by subtracting the level of inhibition predicted as additive by the Loewe model from the actual observed inhibition. Therefore, positive excess values indicate synergy and negative values indicate antagonism. The synergy score for each matrix is shown below each example in gold text. A minimum synergy score of 2.1 was considered the threshold for the combination to be considered synergistic and values over 12 are considered strong synergies. An example of both a strong and a more moderate synergistic interaction are shown for each combination.

numbers are limiting, our data indicate that using LibA with four guides per gene will be sufficient to identify targets in a drug–gene sensitivity screen.

Our simulated analyses indicate that our component libraries are all able to find essential genes or controls with high confidence, and in fact only two guides were required to successfully complete this exercise. Indeed, robust identification of essential genes using a low complexity library can be expected, and is already established in multiple publications.[2,3,37,38] Surprisingly, increasing the guide number in the case of essential gene discovery resulted in a minor increase in variance, most likely owing to the necessary but modest decrease in the ranking performance of guides included in each of the increasingly complex libraries.

The analysis of drop-out genes indicative of sensitization to olaparib provided a surprisingly rich dataset and showed excellent overall concordance with a previous publication.[9] Zimmermann and colleagues[9] exploited an alternative approach for enriching their dataset by simultaneous screening in several cell lines. We identify the RNaseH2 complex as a key hit in our screens, an observation consistent with the results from Zimmermann *et al*.,[9] where the authors directly validated these hits. The substantial overlap of hits identified in our single CRISPR screen with previously published olaparib screens is further compelling evidence that our new component library is working effectively.

We validated some of the hits identified in our pooled CRISPRko screen by combinatorial drug screens in cell line panels with two clinical PARP inhibitors, olaparib and talazoparib. This orthogonal approach delivers rapid initial validation of selective hits in high throughput. Initial validation through this approach enables targets to be considered in terms of their tractability in the clinic. These data also illustrate how well CRISPR screens and high throughput cell panel screens can be used to rapidly validate new, clinically relevant genetic interactions.

Interestingly, the overlap between the hits in distinct cell models, both from this screen and those published previously,[9] indicate that while broad agreement is found between some of the major hits (as discussed above), there remains a high degree of difference between hits found in each cell line background. Although overall concordance between screens is broadly substantially great than that observed in RNA interference screens, for example,[39–41] this observation is a valuable indication that robust conclusions around drug-gene interactions are best made from screens conducted across diverse genetic and lineage backgrounds, to more completely describe the effects. This can be achieved with our fully integrated pooled CRISPRko and high throughput cell panel screening platform.

Overall, our analysis of screening with a new flexible library and hit validation by combinatorial drug screening provides a powerful new approach, particularly well suited to the variable experimental demands of each screening campaign with potentially rapid clinical translation. Hit identification was broadly improved with higher complexity libraries, providing increased confidence and interrogation depth. The lower complexity screens also performed well, indicating that these tools will be poised to support robust hit discovery in future positive selection screening campaigns.

Acknowledgments

The authors thank all members of the screening group for their excellent technical support and Nicola McCarthy for help with reviewing and editing the manuscript.

M.B., D.A.S., and B.C.S.C. conceived the experiments; M.B., M.B.B-Z, G.R.A.M., C.l.S., H.N.P., G.S.T., and S.L. carried out the experiments; S.L. and J.E.M. ran the bioinformatics; and M.B., D.A.S., and B.C.S.C. wrote the paper. All authors reviewed the final version.

Author Disclosure Statement

At the time the experiments were carried out, all authors were employees of Horizon Discovery, Ltd.

Funding Information

No funding was received for this article.

References

1. Hart T, Chandrashekhar M, Aregger M, et al. High-resolution CRISPR screens reveal fitness genes and genotype-specific cancer liabilities. *Cell.* 2015;163:1515–1526. DOI: 10.1016/j.cell.2015.11.015.
2. Dempster JM, Pacini C, Pantel S, et al. Agreement between two large pan-cancer CRISPR-Cas9 gene dependency datasets. *Nat Commun.* 2019;10:5817. DOI: 10.1038/s41467-019-13805-y.
3. Behan FM, Iorio F, Picco G, et al. Prioritization of cancer therapeutic targets using CRISPR–Cas9 screens. *Nature.* 2019;568:511–516. DOI: 10.1038/s41586-019-1103-9.
4. Meyers RM, Bryan JG, Mcfarland JM, et al. Computational correction of copy-number effect improves specificity of CRISPR-Cas9 essentiality screens in cancer cells. *Nat Genet.* 2017;49:1779–1784. DOI: 10.1038/ng.3984.
5. Shalem O, Sanjana NE, Hartenian E, et al. Genome-scale CRISPR-Cas9 knockout screening in human cells. *Science.* 2014;343:84–87. DOI: 10.1126/science.1247005.
6. Le Sage C, Lawo S, Panicker P, et al. Dual direction CRISPR transcriptional regulation screening uncovers gene networks driving drug resistance. *Sci Rep.* 2017;7:1–10. DOI: 10.1038/s41598-017-18172-6.
7. Wang T, Birsoy K, Hughes NW, et al. Identification and characterization of essential genes in the human genome. *Science.* 2015;350:1096–1101. DOI: 10.1126/science.aac7041.
8. Michlits G, Hubmann M, Wu SH, et al. CRISPR-UMI: single-cell lineage tracing of pooled CRISPR-Cas9 screens. *Nat Methods.* 2017;49:1779–1784. DOI: 10.1038/nmeth.4466.
9. Zimmermann M, Murina O, Reijns MAM, et al. CRISPR screens identify genomic ribonucleotides as a source of PARP-trapping lesions. *Nature.* 2018;559:285–289. DOI: 10.1038/s41586-018-0291-z.
10. Szlachta K, Kuscu C, Tufan T, et al. CRISPR knockout screening identifies combinatorial drug targets in pancreatic cancer and models cellular drug response. *Nat. Commun.* 2018;9:4275. DOI: 10.1038/s41467-018-06676-2.

11. Xiao T, Li W, Wang X, et al. Estrogen-regulated feedback loop limits the efficacy of estrogen receptor–targeted breast cancer therapy. *Proc Natl Acad Sci USA.* 2018;115:7869–7878. DOI: 10.1073/pnas.1722617115.
12. Wei L, Lee D, Law CT, et al. Genome-wide CRISPR/Cas9 library screening identified PHGDH as a critical driver for sorafenib resistance in HCC. *Nat Commun.* 2019;10:4681. DOI: 10.1038/s41467-019-12606-7.
13. Chen S, Sanjana NE, Zheng K, et al. Genome-wide CRISPR screen in a mouse model of tumor growth and metastasis. *Cell.* 2015;160: 1246–1260. DOI: 10.1016/j.cell.2015.02.038.
14. Doench JG, Fusi N, Sullender M, et al. Optimized sgRNA design to maximize activity and minimize off-target effects of CRISPR-Cas9. *Nat Biotechnol.* 2016;34:184–191. DOI: 10.1038/nbt.3437.
15. Zhou Y, Zhu S, Cai C, et al. High-throughput screening of a CRISPR/Cas9 library for functional genomics in human cells. *Nature* 2014;509: 487–491. DOI: 10.1038/nature13166.
16. Jost M, Chen Y, Gilbert LA, et al. Combined CRISPRi/a-based chemical genetic screens reveal that rigosertib is a microtubule-destabilizing agent. *Mol Cell.* 2017;68:210–223.e6. DOI: 10.1016/j.molcel.2017.09.012.
17. Arroyo JD, Jourdain AA, Calvo SE, et al. A genome-wide CRISPR death screen identifies genes essential for oxidative phosphorylation. *Cell Metab.* 2016;24:875–885. DOI: 10.1016/j.cmet.2016.08.017.
18. Cross BCS, Lawo S, Archer CR, et al. Increasing the performance of pooled CRISPR–Cas9 drop-out screening. *Sci Rep.* 2016;6:31782. DOI: 10.1038/ srep31782.
19. Blomen VA, Májek P, Jae LT, et al. Gene essentiality and Synthetic Lethality in Haploid Human Cells. *Science*. 2015;350:1092–1096. DOI: 10.1126/science.aac7557.
20. Hart T, Tong AHY, Chan K, et al. Evaluation and design of genome-wide CRISPR/SpCas9 knockout screens. *G3 (Bethesda)* 2017;7:2719–2727. DOI: 10.1534/g3.117.041277.
21. Sanjana NE, Shalem O, Zhang F. Improved vectors and genome-wide libraries for CRISPR screening. *Nat Methods* 2014;11:783–784. DOI: 10.1038/nmeth.3047.
22. Strezoska Ž, Perkett MR, Chou ET, et al. High-content analysis screening for cell cycle regulators using arrayed synthetic crRNA libraries. *J Biotechnol.* 2017;251:189–200. DOI: 10.1016/j.jbiotec.2017.04.017.
23. Chen B, Gilbert LA, Cimini BA, et al. Dynamic imaging of genomic loci in living human cells by an optimized CRISPR/Cas system. *Cell.* 2013;155:1479–1491. DOI: 10.1016/j.cell.2013.12.001.
24. Andrews S. FastQC: A quality control tool for high throughput sequence data. https://www.bioinformatics.babraham.ac.uk/projects/fastqc/ (last accessed November 18, 2019).
25. Wang G, Zimmermann M, Mascall K, et al. Identifying drug-gene interactions from CRISPR knockout screens with DrugZ. *bioRxiv.* 2017 Dec 12. DOI: https://doi.org/10.1101/232736.
26. Colic M, Wang G, Zimmermann M, et al. Identifying chemogenetic interactions from CRISPR screens with DrugZ. *Genome Med.* 2019;11:52. DOI: 10.1186/s13073-019-0665-3.
27. Bean DM, Heimbach J, Ficorella L, et al. EsyN: network building, sharing and publishing. *PLoS One* 2014;9:e106035. DOI: 10.1371/journal.pone.0106035.
28. Toshimitsu U. Identification of combinatorial drugs that synergistically kill both eribulin-sensitive and eribulin-insensitive tumor cells. *Glob J Cancer Ther.* 2015;1:9–17. DOI: 10.17352/gjct.000004.
29. Huang DW, Sherman BT, Lempicki RA. Systematic and integrative analysis of large gene lists using DAVID bioinformatics resources. *Nat Protoc.* 200;4:44–57. DOI: 10.1038/nprot.2008.2119.
30. Lord CJ, Ashworth A. BRCAness Revisited. *Nat Rev Cancer.* 2016;16: 110–120. DOI: 10.1038/nrc.2015.21.
31. Lord CJ, Ashworth A. PARP inhibitors: synthetic lethality in the clinic. *Science*. 2017;355:1152–1158. DOI: 10.1126/science.aam7344.
32. Pan D, Kobayashi A, Jiang P, et al. A major chromatin regulator determines resistance of tumor cells to T cell-mediated killing. *Science.* 2018;359:770–775. DOI: 10.1126/science.aao1710.
33. Li W, Xu H, Xiao T, et al. MAGeCK enables robust identification of essential genes from genome-scale CRISPR/Cas9 knockout screens. *Genome Biol.* 2014;15:554. DOI: 10.1186/s13059-014-0554-4.
34. Mendes-Pereira AM, Martin SA, Brough R, et al. Synthetic lethal targeting of PTEN mutant cells with PARP inhibitors. *EMBO Mol Med.* 2009;1: 315–322. DOI: 10.1002/emmm.200900041.
35. Murai J, Huang SYN, Renaud A, et al. Stereospecific PARP trapping by BMN 673 and comparison with olaparib and rucaparib. *Mol Cancer Ther.* 2014;13:433–443. DOI: 10.1158/1535-7163.MCT-13-0803.
36. Gonçalves E, Segura-Cabrera A, Pacini C, et al. Drug mechanism-of-action discovery through the integration of pharmacological and CRISPR screens. *bioRxiv.* 2020.01.14.905729; DOI: https://doi.org/10.1101/ 2020.01.14.905729.
37. Hart T, Moffat J. BAGEL: a computational framework for identifying essential genes from pooled library screens. *BMC Bioinformatics.* 2016;17:1–7. DOI: 10.1186/s12859-016-1015-8.
38. Doench JG. Am I ready for CRISPR? A user's guide to genetic screens. *Nat Rev Genet.* 2018;19:67–80. DOI: 10.1038/nrg.2017.97.
39. König R, Zhou Y, Elleder D, et al. Global analysis of host-pathogen interactions that regulate early-stage HIV-1 replication. *Cell* 2008;135:49–60. DOI: 10.1016/j.cell.2008.07.032.
40. Zhou H, Xu M, Huang Q, et al. Genome-scale RNAi screen for host factors required for HIV replication. *Cell Host Microbe.* 2008;4:495–504. DOI: 10.1016/j.chom.2008.10.004.
41. Brass AL, Dykxhoorn DM, Benita Y, et al. Identification of host proteins required for HIV infection through a functional genomic screen. *Science.* 2008;319:921–926. DOI: 10.1126/science.1152725.